SPECIAL TOPIC — Acoustics

Improving the performance of acoustic invisibility with multilayer structure based on scattering analysis*

Chen Cai(蔡琛)[1], Yin Yuan(袁樱)[2], Wei-Wei Kan(阚威威)[3], Jing Yang(杨京)[1], and Xin-Ye Zou(邹欣晔)[1,†]

[1] Key Laboratory of Modern Acoustics, MOE, and Institute of Acoustics, Department of Physics, Nanjing University, Nanjing 210093, China
[2] The School of Mathematics and Physics, Jiangsu University of Technology, Changzhou 213001, China
[3] School of Science, Nanjing University of Science and Technology, Nanjing 210094, China

(Received 29 April 2016; revised manuscript received 23 June 2016; published online 25 October 2016)

In this paper, acoustic scattering from the system comprised of a cloaked object and the multilayer cloak with only one single pair of isotropic media is analyzed with a recursive numerical method. The designed acoustic parameters of the isotropic cloak media are assumed to be single-negative, and the resulting cloak can reduce acoustic scattering from an acoustic sensor while allowing it to receive external information. Several factors that may influence the performance of the cloak, including the number of layers and the acoustic dissipation of the medium are fully analyzed. Furthermore, the possibility of achieving acoustic invisibility with positive acoustic parameters is proposed by searching the optimum value in the parameter space and minimizing the scattering cross-section.

Keywords: metamaterials, acoustic cloaking, scattering, invisibility

PACS: 43.20.–f, 43.35.+d, 62.90.+k **DOI:** 10.1088/1674-1056/25/12/124302

1. Introduction

In 2006, Pendry *et al.* proposed the concept of transformation optics, and used this coordinate transformation technique to design an invisibility cloak for electromagnetic waves.[1] Ever since them, the coordinate transformation technique has attracted worldwide attention. Such a method was extended to the field of acoustics by Cummer and Schurig in 2006.[2] Since then there has been growing interest in acoustic invisibility[3–9] due to the possibility of hiding objects from detecting the acoustic signals, which may lead to applications in a variety of practical situations such as noninvasive acoustic sensors.

Recent research suggested that it is possible to "cancel" the cloaked object as well as to share information from its surroundings by using the complementary objects made of a double-negative medium (DNM).[10] While DNM has been proposed and demonstrated by using acoustic metamaterials,[11–15] the corresponding unit cells are usually related to a resonate effect and consequently are only effective in narrow band. Besides, the resonance-induced dissipation will inevitably harm the performance of the resulting device. Therefore the invisibility cloak based on DNM would be less practical for acoustic waves. Zhu *et al.* proposed the superlens cloaking by using single-negative medium (SNM) in 2011.[16] Compared with the DNM device, the invisibility cloak based on SNM would generally be easy to fabricate and effective to work in broader bandwidth.[17] Although the superlens cloaking by Zhu *et al.* is proved to be effective in reducing acoustic scattering from an acoustic sensor, such a device is composed of inhomogeneous anisotropic media which require, even in a reducible way, a large number of isotropic media with different parameters, and thus bringing the difficulty in fabricating it. Later, Zhu *et al.*[18] revised their folding transformation scheme and simplified the cloaking method, in which only three types of SNMs are needed. Xu *et al.*[19] further simplified the superlens fabrication process, and in their scheme, only one single pair of isotropic media is required for reducing the acoustic scattering.

In this paper, a recursive numerical method of calculating the acoustic scattering from the structure with a homogeneous isotropic multilayer shell is given in detail, and based on this method the SNM superlens cloaking is fully analyzed. The influences of several factors that may hinder the performance of the cloak, including the number of layers, acoustic dissipation of the media, etc., are investigated. According to the results above, we further investigate the possibility of achieving a positive parameter invisibility device, by searching, in the parameter space, for the optimum value that can render the scattering cross-section minimum.

The rest of the present article is organized as follows. In Section 2, we first introduce the theory of superlens cloaking

*Project supported by the National Natural Science Foundation of China (Grant Nos. 11274168, 11374157, 11174138, 11174139, 11222442, and 81127901) and the National Basic Research Program of China (Grant Nos. 2010CB327803 and 2012CB921504).

†Corresponding author. E-mail: xyzou@nju.edu.cn

© 2016 Chinese Physical Society and IOP Publishing Ltd

and then give the theoretical formulation for scattering analyses with the recursive numerical method. In Section 3, we present in detail the numerical results for the cloaking performance in various situations, analyze the factors that may influence the invisibility effect, and give an example of an invisibility cloak based on scattering cancellation. Finally, we draw some conclusions from the present studies in Section 4.

2. Theoretical methods

2.1. Theory of superlens cloaking

For simplicity, we restrict the problem to a two-dimensional (2D) case. A sketch of the folding space transformation is shown in Figs. 1(a) and 1(b). During space transformation, the space $A+C$ is transformed into the space $A'+C$, and space B' filled with complementary media is used to keep the continuity in the acoustic field. The unprimed and primed coordinate are used to represent the virtual space and the physical space, respectively. For the mapping A–A' and C–C, the transforming equations can be written as $r=f(r')$, $\theta=\theta'$, with $f(r)=(a'/a)r$, $(r<a)$, and $f(r)=r$, $(r>b)$, respectively. According to transformation acoustic theory, the bulk modulus and inverse mass density tensor in the transformed space are given as $\kappa'(x')=\kappa(x)\det(H)$ and $\rho'^{-1}(x')=H\rho^{-1}(x)H^{\mathrm{T}}/\det(H)$, respectively. Here, H is the Jacobian transformation tensor with the components as $H_{ij}=(h_{x_i'}/h_{x_j})\partial x_i'/\partial x_j$, in which h_{x_i} and $h_{x_i'}$ are the scale factors in virtual space and physical space, respectively. If the virtual space is occupied by a homogeneous isotropic medium with bulk modulus κ_0 and mass density ρ_0, then the material parameters in medium A' become $\kappa'=(a'/a)^2\kappa$ and $\boldsymbol{\rho}'=\rho_0\boldsymbol{I}$.

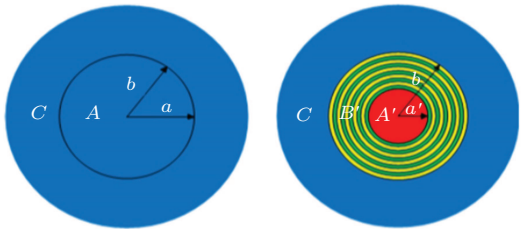


Fig. 1. (color online) Sketches of the folding space mapping: (a) the virtual space consists of the bulk of the background medium; (b) the real space consists of three parts: circular area A', annular shell B', and the domain C outside. B' is further divided by N bilayers with $2N$ rings. The mapping relationship is shown as $A\leftrightarrow A', C\leftrightarrow C'..B'_{2n-1}\leftrightarrow B'_{2n}$ $(n=1,2,...,N)$.

Now we focus on the annular shell B' which is divided into N bilayers $[(B'_1B'_2),(B'_3B'_4),\ldots,(B'_{2N-1}B'_{2N})]$ with the same thickness, and the two rings in each bilayer can be obtained through the folding transformation to meet the spatial continuity requirement. Thus the thickness of each bilayer can be obtained as

$$s=\frac{b-a'}{N}. \tag{1}$$

The n-th bilayer $(B'_{2n-1}B'_{2n})$ is at the position $d_{n-1}\le r'<d_n$, $d_n=a'+ns$ $(n=1,2,...,N)$. In order to avoid anisotropy, the radial section of the two rings is selected as

$$r'=f(r)=\frac{d_{n-1}d_n}{r}=\frac{\delta_n^2}{r},\ \ (d_{n-1}\le r<\delta_n), \tag{2}$$

where δ_n is the position of the dividing line between the two small rings, and $\delta_n^2=d_{n-1}d_n$. As a result, $\alpha=\partial f(r)/\partial r=-\delta_n^2/r^2$ and $\eta=f(r)/r=\delta_n^2/r^2$. The relationship between the material parameters in B'_{2n-1} and B'_{2n} is given as

$$\rho'_{2n-1}=-\rho'_{2n},\ \ \kappa'_{2n-1}=-\left(\frac{r'}{\delta_n}\right)^4\kappa'_{2n}. \tag{3}$$

When N is large enough, the thickness of each bilayer tends to be 0, so

$$\begin{aligned}\delta_n &= \sqrt{d_{n-1}d_n}\\ &= \sqrt{[a'+(n-1)s](a'+ns)}\\ &\approx a'+\frac{2n-1}{2}s\\ &= \frac{d_n+d_{n-1}}{2}.\end{aligned} \tag{4}$$

Since the dividing line is in the middle of the bilayer, the thickness values of $2N$ rings are the same. Meanwhile, when the thickness of each bilayer tends to be 0, the radial coordinates of all points in each small ring are almost equal, that is $r'\approx\delta$, so equation (3) is rewritten as

$$\rho'_{2n-1}=-\rho'_{2n},\ \ \kappa'_{2n-1}\approx-\kappa'_{2n}. \tag{5}$$

The proposed structure can thus be realized with a pair of complementary SNMs, in which the parameters are independent of those of the background medium C or the medium A'.

2.2. Scattering analysis

In order to present the recursive procedure clearly, we begin with the case of only one single cylindrical scattering object. The analysis focuses on acoustic waves propagating along the cross section of a homogeneous infinite cylinder in a host medium. Cylindrical coordinates (r,θ,z) are used throughout the analysis, and the material is assumed to be isotropic. The wave vector is in the plane $(r-\theta)$, and the wave-front extends infinitely along the z direction. We assume that the external incident acoustic wave can be described as $p^0_{\mathrm{inc}}=\sum_n\alpha_n^0\mathrm{J}_n(k_0r)\,\mathrm{e}^{in\theta}$, and the only scattering object is marked as number 1. So the corresponding incident, scattered and transmitted waves can be expanded into $p^1_{\mathrm{inc}}=\sum_n\alpha_n^1\mathrm{J}_n(k_0r)\,\mathrm{e}^{in\theta}$, $p^1_{\mathrm{scr}}=\sum_n\beta_n^1H_n^{(1)}(k_0r)\,\mathrm{e}^{in\theta}$, and $p^1_{\mathrm{tra}}=\sum_n\gamma_n^1\mathrm{J}_n(k_1r)\,\mathrm{e}^{in\theta}$, where k_0 and k_1 are the wave vectors for the host medium and the scattering object, respectively; J_n is the Bessel function; $\mathrm{H}_n^{(1)}$ is the Hankel function of the first kind; α_n^0, α_n^1, β_n^1, and γ_n^1 are undetermined coefficients. For this scattering problem, $p^1_{\mathrm{inc}}=p^0_{\mathrm{inc}}$ and $\alpha_n^1=\alpha_n^0$. The radius

of the infinite cylinder is a. According to the interface continuity condition, we can obtain

$$\begin{aligned} &p^1_{\rm inc}\big|_{r=a}+p^1_{\rm scr}\big|_{r=a}=p^1_{\rm tra}\big|_{r=a},\\ &\frac{1}{\rho_0}\left(\frac{\partial p^1_{\rm inc}}{\partial r}\bigg|_{r=a}+\frac{\partial p^1_{\rm scr}}{\partial r}\bigg|_{r=a}\right)=\frac{1}{\rho_1}\left(\frac{\partial p^1_{\rm tra}}{\partial r}\bigg|_{r=a}\right), \end{aligned} \tag{6}$$

where ρ_0 and ρ_1 are the density of the host medium and the scattering object, respectively. Then, we can obtain

$$\beta^1_n=R^1_n\alpha^1_n,\ \ \gamma^1_n=T^1_n\alpha^1_n, \tag{7}$$

and it can also be expressed in the matrix form

$$\boldsymbol{\beta}^1=\boldsymbol{R}^1\boldsymbol{\alpha}^1=\boldsymbol{R}^1\boldsymbol{\alpha}^0,\ \ \boldsymbol{\gamma}^1=\boldsymbol{T}^1\boldsymbol{\alpha}^1=\boldsymbol{T}^1\boldsymbol{\alpha}^0, \tag{8}$$

where $\boldsymbol{R}^1$ is the scattering matrix and $\boldsymbol{T}^1$ the transmission matrix. It can be seen that the scattering matrix and the transmission matrix are diagonal matrices because of the symmetrical scattering object. According to the asymptotic expression for the Hankel function for large arguments, the far-field scattering pressure can be written as[20]

$$\begin{aligned} \lim_{r\to\infty}|p_{\rm scr}| &= \lim_{r\to\infty}\left|\sum_n\beta_n{\rm H}^{(1)}_n(k_0r)\,{\rm e}^{{\rm i}n\theta}\right|\\ &=\left|\sum_n\beta_n\sqrt{\frac{2}{\pi k_0r}}\,{\rm e}^{{\rm i}(k_0r-n\pi/2-\pi/4)}\,{\rm e}^{{\rm i}n\theta}\right|\\ &=\sqrt{\frac{2}{\pi k_0r}}\left|\sum_n\beta_n\,{\rm e}^{{\rm i}n(\theta-\pi/2)}\right|\\ &\equiv\sqrt{\frac{2}{\pi k_0r}}f(\theta), \end{aligned} \tag{9}$$

where $p_{\rm scr}$ is the far-field scattering pressure, and the scattering directional factor $f(\theta)=|\sum_n\beta_n\,{\rm e}^{{\rm i}n(\theta-\pi/2)}|$. Therefore, the total scattering cross section of the scattering object is

$$\sigma=\frac{2}{\pi k_0}\int_0^{2\pi}|f(\theta)|^2\,{\rm d}\theta. \tag{10}$$

We show part of the multilayer structure in the first quadrant in Fig. 2. Layers and boundaries are numbered consecutively inward. It is assumed that there are N layers with the host as layer 0 and the innermost core as layer N. The acoustic impedance of layer j is $z_j=\rho_jc_j$, and the corresponding wave number and radius are k_j and a_j, respectively.

The acoustic field can be regarded as a superposition of the standing wave (corresponding to the Bessel function) and the scattered wave outward (corresponding to the Hankel function of the first kind). For instance, in the host medium, it is expressed as

$$\begin{aligned} p_0 &= p_{0\rm inc}+p_{0\rm scr}\\ &=\sum_n\alpha_{0,n}{\rm J}_n(k_0r)\,{\rm e}^{{\rm i}n\theta}+\sum_nR_n\alpha_{0,n}{\rm H}^{(1)}_n(k_0r)\,{\rm e}^{{\rm i}n\theta}. \end{aligned} \tag{11}$$

In the innermost layer N, the standing wave field can be obtained by

$$p_N=p_{N\rm trs}=\sum_nT_{N,n}\alpha_{0,n}{\rm J}_n(k_Nr)\,{\rm e}^{{\rm i}n\theta}. \tag{12}$$

In all other layers from layer1 to layer $N-1$, the acoustic field is

$$\begin{aligned} p_j &= p_{j\rm sta}+p_{jf}\\ &=\sum_nS_{j,n}\alpha_{0,n}{\rm J}_n(k_jr)\,{\rm e}^{{\rm i}n\theta}\\ &\quad+\sum_nF_{j,n}\alpha_{0,n}{\rm H}^{(1)}_n(k_jr)\,{\rm e}^{{\rm i}n\theta}, \end{aligned} \tag{13}$$

where $S_{j,n}$ and $F_{j,n}$ are the coefficients for standing wave field and scattered wave field, $j=1,\ldots,N-1$.

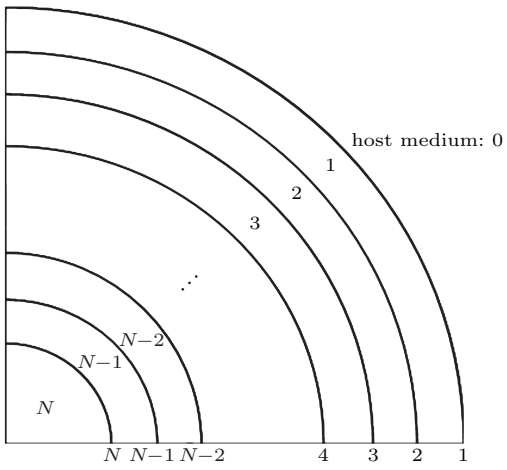


Fig. 2. First-quadrant cross section of the multilayer structure.

2.3. Recursive approach

If we already know the incident wave, that is, the value of α_{0n} is given, then there are two general approaches to determining the acoustic scattering field. One is to list all the continuity conditions at all the interfaces, and solve the undetermined coefficient at one time;[5] the other is the recursive approach,[21] which is employed in this paper. The general idea of this recursive method is similar to the transfer matrix method.[22,23] Consider that the acoustic wave in layer $j-1$ impinges onto layer j (where $j=1,...,N$), the incident, reflected and transmitted waves can be written as $\sum_nA_n{\rm J}_n(k_{j-1}r)\,{\rm e}^{{\rm i}n\vartheta}$, $\sum_nR^i_{j-1,n}A_n{\rm H}^{(1)}_n(k_{j-1}r)\,{\rm e}^{{\rm i}n\vartheta}$, and $\sum_nT^i_{j-1,n}A_n{\rm J}_n(k_{j-1}r)\,{\rm e}^{{\rm i}n\vartheta}$, respectively, where the superscript i signifies that the direction of the incident wave is inward, and the subscripts $j-1$ indicate that the incident wave is in medium $j-1$. The coefficients of the reflected and transmitted coefficients, respectively, are

$$R^i_{j-1,n}=-\frac{z_{j-1}{\rm J}'_n(k_ja_j){\rm J}_n(k_{j-1}a_j)-z_j{\rm J}_n(k_ja_j){\rm J}'_n(k_{j-1}a_j)}{z_{j-1}{\rm J}'_n(k_ja_j){\rm H}^{(1)}_n(k_{j-1}a_j)-z_j{\rm J}_n(k_ja_j){\rm H}^{(1)\prime}_n(k_{j-1}a_j)},$$

$$T^{i}_{j-1,n} = -\frac{2\mathrm{i}}{\pi k_0 a_j} \cdot \frac{z_j}{z_{j-1}\mathrm{J}'_n(k_j a_j)\mathrm{H}^{(1)}_n(k_{j-1}a_j) - z_j \mathrm{J}_n(k_j a_j)\mathrm{H}^{(1)\prime}_n(k_{j-1}a_j)}, \tag{14}$$

where z_j and z_{j-1} are the acoustic impedances of their corresponding layers.

On the other hand, when the wave travels from layer j towards layer $j-1$ (where $j = 1,...,N$), the incident, reflected and transmitted waves can be written as $\sum_n A_n \mathrm{H}^{(1)}_n(k_j r)\,\mathrm{e}^{\mathrm{i}n\theta}$, $\sum_n R^{\mathrm{o}}_{j,n} A_n \mathrm{J}_n(k_{j-1}r)\,\mathrm{e}^{\mathrm{i}n\theta}$, and $\sum_n T^{\mathrm{o}}_{j,n} A_n \mathrm{H}^{(1)}_n(k_j r)\,\mathrm{e}^{\mathrm{i}n\theta}$, respectively, where superscript o signifies that the direction of the incident wave is outward, the subscript j indicates the incident wave is in medium j. We can obtain coefficients of reflected and transmitted waves by solving boundary equations:

$$\begin{aligned} R^{\mathrm{o}}_{j,n} &= -\frac{z_{j-1}\mathrm{H}^{(1)\prime}_n(k_j a_j)\mathrm{H}^{(1)}_n(k_{j-1}a_j) - z_j \mathrm{H}^{(1)}_n(k_j a_j)\mathrm{H}^{(1)\prime}_n(k_{j-1}a_j)}{z_{j-1}\mathrm{J}'_n(k_j a_j)\mathrm{H}^{(1)}_n(k_{j-1}a_j) - z_j \mathrm{J}_n(k_j a_j)\mathrm{H}^{(1)\prime}_n(k_{j-1}a_j)}, \\ T^{\mathrm{o}}_{j,n} &= -\frac{2\mathrm{i}}{\pi k_0 a_j} \frac{z_{j-1}}{z_{j-1}\mathrm{J}'_n(k_j a_j)\mathrm{H}^{(1)}_n(k_{j-1}a_j) - z_j \mathrm{J}_n(k_j a_j)\mathrm{H}^{(1)\prime}_n(k_{j-1}a_j)}. \end{aligned} \tag{15}$$

When only the innermost layer exists, there are two media in the space, where the scattering object is medium N with radius a_N and the host material is medium $N-1$. When the incident wave is given as $\sum_n A_n \mathrm{J}_n(k_{N-1}r)\,\mathrm{e}^{\mathrm{i}n\theta}$, the reflected and transmitted waves are

$$\sum_n R^{i}_{N-1,n} A_n \mathrm{H}^{(1)}_n(k_N r)\,\mathrm{e}^{\mathrm{i}n\theta}, \tag{16}$$

$$\sum_n T^{i}_{N-1,n} A_n \mathrm{J}_n(k_{j-1} r)\,\mathrm{e}^{\mathrm{i}n\theta}. \tag{17}$$

The total reflection coefficient in layer N is represented by $R_{N,n} = R^{i}_{N-1,n}$, which equals the reflection coefficient of layer N since there is only one layer. Then the outermost host medium is changed into medium $N-2$, and the scattering object of medium N with radius a_N is wrapped by layer $N-1$ with outer radius a_{N-1}, thus an effective dual-layer structure can be obtained. The acoustic wave will be reflected back and forth in layer $N-1$, and we can obtain the reflection and transmission coefficients from Eqs. (14) and (15).

Supposing that the incident wave has the form of $\sum_n A_n \mathrm{J}_n(k_{N-2}r)\,\mathrm{e}^{\mathrm{i}n\theta}$. The wave reflected from boundary $N-1$ into medium $N-2$ is

$$\sum\nolimits_n (R^{i}_{N-2,n} + M_{N-1,n} R_{N,n} T^{\mathrm{o}}_{N-1,n}) A_n \mathrm{H}^{(1)}_n(k_{N-2}r)\,\mathrm{e}^{\mathrm{i}n\theta}.$$

Thus the total reflection coefficient in layer $N-1$ can be written as $R_{N-1,n} = R^{i}_{N-2,n} + M_{N-1,n} R_{N,n} T^{\mathrm{o}}_{N-1,n}$. The multiple scattering factor M in layer $N-1$ is $M_{N-1,n} = T^{i}_{N-2,n}(1 - R_{N,n} R^{\mathrm{o}}_{N-1,n})^{-1}$, and the transmitted wave in medium N can be written as

$$\sum_n M_{N-1,n} T^{i}_{N-1} A_n \mathrm{J}_n(k_N r)\,\mathrm{e}^{\mathrm{i}n\theta}. \tag{18}$$

The standing wave field in medium $N-1$ can be written as $\sum_n M_{N-1,n} A_n \mathrm{J}_n(k_{N-1}r)\,\mathrm{e}^{\mathrm{i}n\theta}$. The outgoing scattering field in medium $N-1$ can be written as $\sum_n M_{N-1,n} R_{N,n} A_n \mathrm{H}^{(1)}_n(k_{N-1}r)\,\mathrm{e}^{\mathrm{i}n\theta}$. Comparing Eq. (17) with Eq. (18), we can see that the incident wave in layer N changes from $\sum_n A_n \mathrm{J}_n(k_{N-1}r)\,\mathrm{e}^{\mathrm{i}n\theta}$ to $\sum_n M_{N-1,n} A_n \mathrm{J}_n(k_{N-1}r)\,\mathrm{e}^{\mathrm{i}n\theta}$, which is the standing wave field in layer $N-1$ by adding a new shell.

According to the method above, the recursion moves outward in the descending direction of j until the outermost host medium becomes an actual host medium, and then we can obtain the whole distribution of acoustic wave field of the multilayered scattering structure. The details of this solution procedure are as follows.

First, from the innermost layer, the multiple scattering factor $M_{j,n}$ and total reflection coefficient $R_{j,n}$ can be obtained as

$$M_{j,n} = T^{i}_{j-1,n}(1 - R_{j+1,n} R^{\mathrm{o}}_{j,n})^{-1} \quad (j = N-1, N-2, ..., 1), \tag{19}$$

$$R_{j,n} = R^{i}_{j-1,n} + M_{j,n} R_{j+1,n} T^{\mathrm{o}}_{j,n} \quad (j = N-1, N-2, ..., 1). \tag{20}$$

The recursion moves outward in the descending direction of j, where $R_{N,n}$ is defined by $R_{N,n} = R^{i}_{N-1,n}$. The total reflection coefficient of the multilayer structure is

$$R_n = R_{1,n}. \tag{21}$$

Then we calculate the coefficient of the wave in the intermediate layer of the scattering object, and the coefficient of the standing wave in layer j is

$$S_{j,n} = \prod_{i=1}^{j} M_{i,n} \quad (j = 1, 2, ..., N-1). \tag{22}$$

The coefficient of the outgoing wave propagating from the core in layer j is

$$F_{j,n} = R_{j+1,n} S_{j,n} \quad (j = 1, 2, ..., N-1). \tag{23}$$

Finally, we can obtain the transmission coefficient of the innermost layer as

$$T_{N,n} = T^{i}_{N-1} S_{N-1,n}. \tag{24}$$

For the cylindrical multilayered structure under investigation in this paper, the acoustic field calculation by other methods may lead to singular values when the material parameters

of adjacent layers are of substantial difference and the number of the layers becomes large. The proposed method in this paper can solve such problems more efficiently and accurately. Furthermore, the total scattering cross section of the structure is easy to obtain with this method, providing convenience in evaluating the performance of the invisibility cloak and the possibility of a new design approach.

3. Numerical results and discussion

Here, the capability of the multilayered shell structure for reducing the acoustic scattering from a cylindrical sensor system in the 2D problem is demonstrated by using the method above. The background medium is chosen to be water with $\rho_0 = 998$ kg/m^3 and $\kappa_0 = 2.19$ GPa. The material parameters of the SNM are $\rho_\alpha = \rho_0$, $\kappa_\alpha = -\kappa_0$, and $\rho_\beta = -\rho_0$, $\kappa_\beta = \kappa_0$. The whole sensor system is regarded as being a scattering object with radius $a' = 1$ cm, in which the effective mass density and the bulk modulus are $\rho_s = \rho_0$ and $\kappa_s = (4/9)\kappa_0$, respectively. The ratio between the outer radius b and the inner radius a' of the annular shell is $b/a' = \sqrt{\kappa_0/\kappa_s} = 1.5$. Figures 3(c) and 3(d) show the normalized acoustic pressure distributions of a bare sensor system illuminated by a plane wave propagating from the left side and a cylindrical wave generated by an infinite line source located at (−3.75 cm, 0 cm), respectively. The wavelengths of the plane wave and the cylindrical wave are chosen to be 0.5 cm. It can be seen that the two acoustic pressure wave fields are strongly disturbed, which leads to a shadow region behind the sensor system and considerable backward reflections. For comparison, figures 3(a) and 3(b) show the result for the sensor system wrapped in a 10-SNM layer shell. It can be found that the disturbance caused by the presence of the sensor system wrapped in the proposed

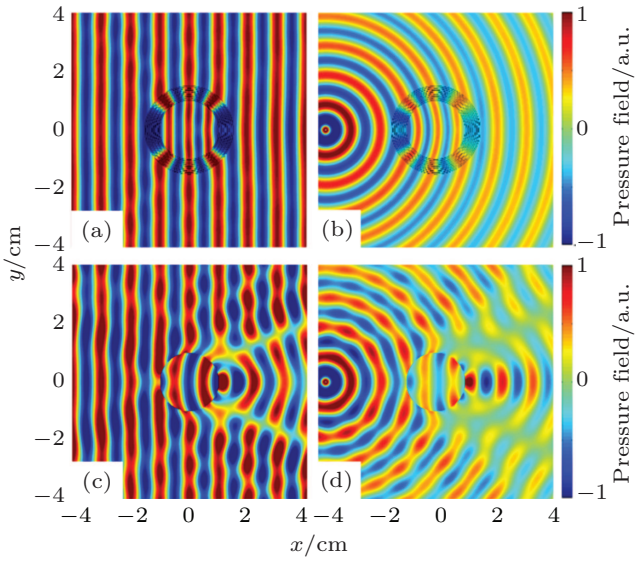


Fig. 3. (color online) Normalized acoustic pressure fields for the plane wave source [(a) and (c)] and for cylindrical wave source [(b) and (d)]. The scattering object is protected by the 10-layer shell ((a) and (b)), and unprotected ((c) and (d)). The unit a.u. is short for arb. units.

structure is negligible. The incident wave can penetrate into the sensor region without changing the wavefront shape.

In order to quantitatively analyze the concealment effect of the proposed structure on the acoustic sensor, and compare the performances of the cloaking shells with different numbers of layers, the variation of total scattering cross-section with the number of layers increasing (up to $N = 100$) is computed, and the results are shown in Fig. 4. As we can see, when the scattering object is wrapped with only two layers (a pair of SNMs), the total scattering cross section is larger than that in the case without the cloak. The reason is that the thickness of each layer of SNM is only half the wavelength and the layer thickness does not meet the subwavelength requirement. However when the number of layers is more than four (two pairs of SNMs), the total scattering cross section of the structure is reduced by one order of magnitude. Meanwhile, the total scattering cross section decreases monotonically as the number of layers of the multilayer structure further increases.

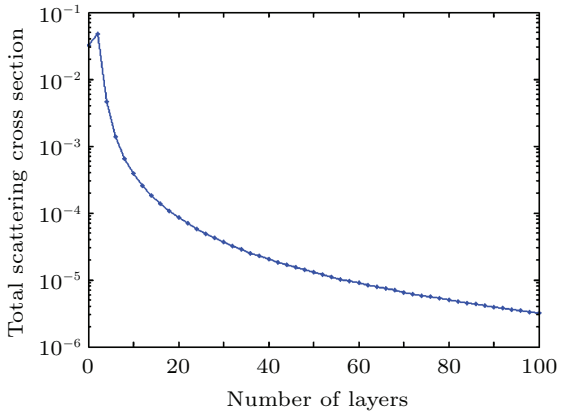


Fig. 4. (color online) Relationship between the total scattering cross section of the structure and the number of layers of the multilayer structure.

Now we consider the case where the equivalent density of the scattering object (bare sensor) is not equal to that of the background medium. According to transformation acoustic theory, the phase matching and impedance matching are established at the same time only when the equivalent density of the scatter is equal to that of the surrounding environment. However, as is well known, the phase matching is more important in those structures. Therefore, on the premise of guaranteeing the phase matching, the impedance matching can be sacrificed to some extent to adapt to the unequal density between the scatter and background medium. So we multiply both the density ρ_s and bulk modulus κ_s by a robust factor ξ. It can be seen from Fig. 5 that the multilayer structure composed of complementary medium can still reduce the scattering by one order of magnitude when $0.5 \leq \xi \leq 2$.

Further, we calculate the acoustic field distribution when ξ values are 0.5 and 2 as shown in Fig. 6. As expected, for both cases, the scattered field is still suppressed by the multilayered structure, which agrees well with the result shown in

Fig. 5. Figures 6(a) and 6(c) each show the normalized acoustic pressure distribution of a bare sensor system illuminated by the plane wave propagating. The wavelength is 0.5 cm. It can be seen that the two acoustic pressure wave fields are strongly disturbed. A comparison of the results in Fig. 6(b) with those in Fig. 6(d) shows the result for the reduced cloak shell, although neither of the wave fronts in Figs. 6(b) and 6(d) is as flat as that of the plane wave.

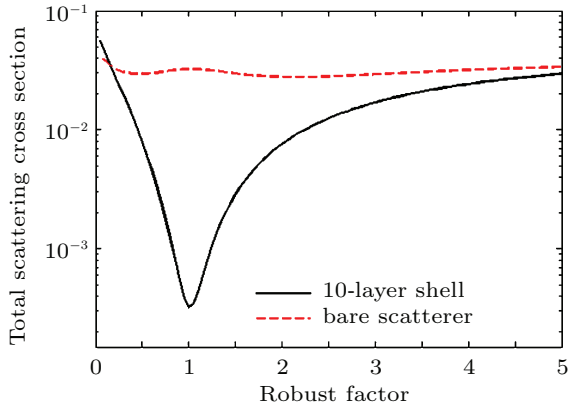


Fig. 5. (color online) Relationships between the total scattering cross section and the robustness factors for the cases of only a bare scatter (dotted curve) and the 10-layer shell scatter (solid curve).

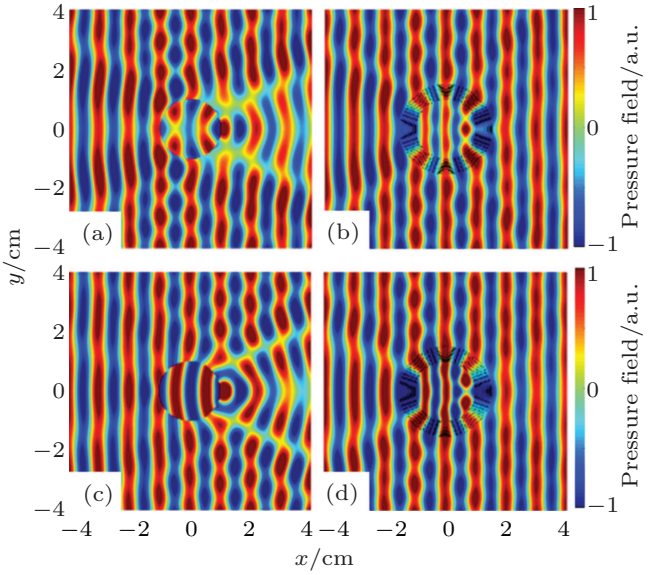


Fig. 6. (color online) Acoustic pressure field distributions when the robust factor ξ values are respectively 0.5 ((a) and (b)) and 2 ((c) and (d)) for the cases of only scatter ((a) and (c)), and a scatter wrapped in a 10-SNM layer shell ((b) and (d)).

According to the previous derivation process, it can be found that the selection of single negative material has no bearing on the parameters of the background medium and the scatter. Here, we investigate the scatterings of the multilayer structure under different material parameters of SNM. We consider two cases: $\rho_\alpha = -3\rho_0$, $\kappa_\alpha = 2\kappa_0$, $\rho_\beta = 3\rho_0$, $\kappa_\beta = -2\kappa_0$, and $\rho_\alpha = -0.5\rho_0$, $\kappa_\alpha = 0.3\kappa_0$, $\rho_\beta = -0.5\rho_0$, $\kappa_\beta = -0.3\kappa_0$. The corresponding acoustic field distributions are shown in Fig. 7.

As we can see from Fig. 7, the scattering becomes strong when none of the absolute values of the material parameters of SNM is equal to its counterpart of the background medium. But most of the scatterings can be suppressed by the multilayer structure, and these scatterings can be eliminated by increasing the number of layers.

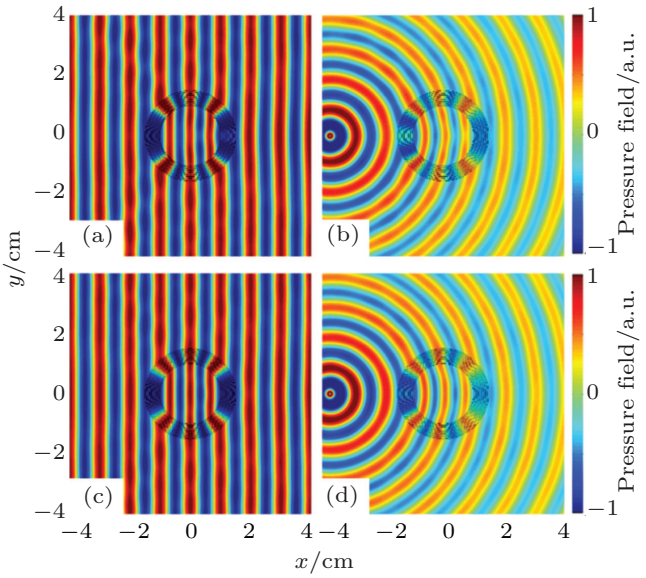


Fig. 7. (color online) Acoustic field distributions when none of the absolute values of the material parameters of SNM is equal to its counterpart of the background medium. In panels (a) and (b): $\rho_\alpha = -\rho_\beta = -3\rho_0$ and $\kappa_\alpha = -\kappa_\beta = 2\kappa_0$; in panels (c) and (d): $\rho_\alpha = -\rho_\beta = -0.5\rho_0$ and $\kappa_\alpha = -\kappa_\beta = 0.3\kappa_0$.

Since single negative material achieved by metamaterial structure inevitably produces dissipation, it is necessary to study the scattering of the multilayer structure with dissipation in SNM. So we add a positive imaginary part to the mass density to describe the dissipation in SNM. Then the mass density used in calculation is $\rho_\alpha = (-1+\mathrm{i}d)\rho_0$, $\rho_\beta = (1+\mathrm{i}d)\rho_0$, where d is the dissipation factor. We calculate the variation of the total scattering cross section when the dissipation coefficient changes, and the results are shown in Fig. 8. It can be found that the multilayer structure composed of complementary media can still reduce the scattering by an order of magnitude when the dissipation reaches up to 10%.

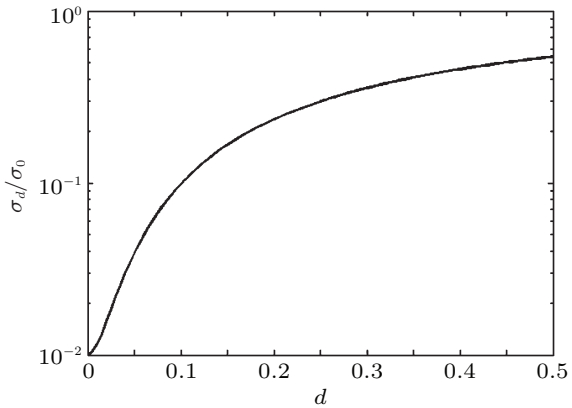


Fig. 8. Relation between the total scattering cross section ratio and the dissipation factor, where σ_0 represents the total scattering cross section of the scatter, σ_d denotes the total scattering cross section of the multilayer structure consisting of the scatter wrapped in a single negative lossy medium.

The corresponding acoustic pressure distributions are shown in Fig. 9 when the dissipation factor values are 5% and 10% respectively. The backscattering is almost zero when dissipation exists, but there exist some scatterings on the other side of the structure. The amplitude of scattering increases as dissipation increases.

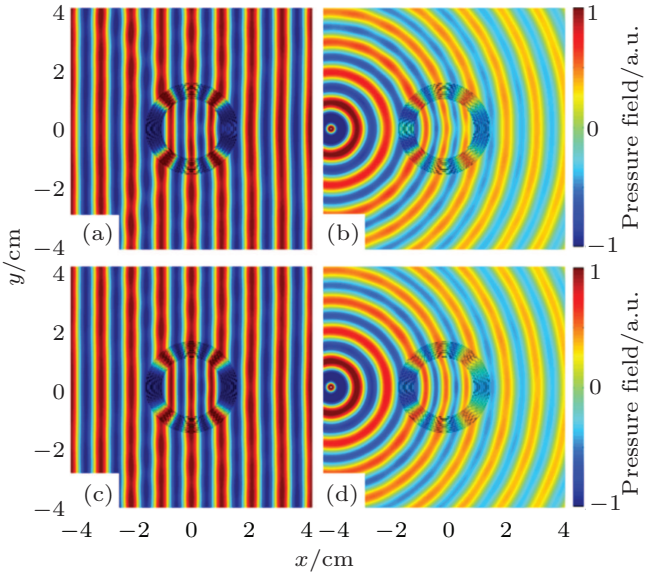


Fig. 9. (color online) Acoustic pressure field distributions when dissipation exists in the multilayer structure consisting of SNM. The dissipation factors are 5% ((a) and (b)) and 10% ((c) and (d)) respectively.

The previous cloaking devices are designed according to the superlens cloaking theory, and analyzed with the scattering method. In the following we will show the possibility of the invisibility cloak design with the scattering method. As shown above, the scattering cross section is easy to obtain with this scattering method, by searching, in the realizable acoustic parameter space, for the optimum value of the cloaking shell that can make the sensor undetectable to the signals, and the scattering-cancellation-type cloak can be obtained. It is assumed that the sensor can be homogenized as a soft effective medium with acoustic parameters of $0.13\rho_0$, $0.15\kappa_0$, with radius of 0.5 cm. For the case without the cloak, the scattering field of this sensor excited by a plane wave source or cylindrical wave source with a wave length of 1 cm are shown in Figs. 10(a) and 10(b) respectively. The acoustic back scattering and shadow area can be clearly observed.

For simplicity, we only use two layers with the same thickness, i.e., 0.2 cm for cloaking, in which case the superlens cloaking method does not work effectively as shown in Fig. 3. The parameter space is assumed to be $0.05\rho_0 \leq \rho \leq 3\rho_0$, $0.05\kappa_0 \leq \kappa \leq 3\kappa_0$. The optimized parameter values are $\rho_\alpha = 0.5\rho_0$, $\kappa_\alpha = 0.38\kappa_0$, $\rho_\beta = 0.13\rho_0$, and $\kappa_\beta = 0.18\kappa_0$. The scattering cross section with these cloak layers decreases down to approximately 2% of the value for the case without the cloak. To verify the performance of this cloak, the acoustic fields for the sensor with the cloak are calculated and shown in Figs. 10(c) and 10(d). It can be seen that the scattering from the sensor and the corresponding shadow area are both cancelled, with the field for plane wave source or cylindrical wave source in free space recovered.

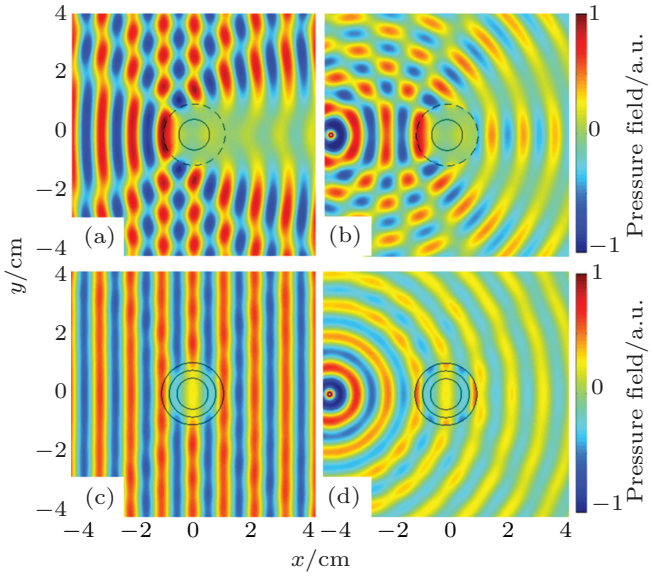


Fig. 10. (color online) Normalized acoustic pressure fields for the plane wave source ((a) and (c)) and cylindrical wave source ((b) and (d)). The scattering sensor is protected by the 2-layer shell ((c) and (d)), and unprotected shell ((a) and (b)) separately.

4. Conclusions

In this paper, the recursive numerical method is employed to study the cylindrical multilayered system and reduces the scattering from an acoustic sensor while allowing it to receive external information. The acoustic pressure field is obviously disturbed by the scattering of the bare sensor system, and the scattering can be cancelled when the sensor system is wrapped in a 10-SNM layer shell. We calculate the acoustic pressure fields in various cases. First, we analyze the scattering characteristics of the cloaking shell with different numbers of bilayers, the total scattering cross section of the structure decreases as the number of bilayers increases. Then we consider the case where the equivalent density of the bare sensor is not equal to the background medium. As expected, the scattered field can still be suppressed by the multilayered shell in this case. Further, we investigate the effect of the SNM parameter on the scattering field. When none of the absolute values of the material parameters of SNM is strictly equal to its counterpart of the background medium, the scattering of the acoustic pressure field emerges, but the scattering can still be suppressed by the multilayer shell. Finally we find that the backscattering nearly approaches to zero when acoustic dissipation induced by SNM is not very strong and some scatterings happen on the other side of the structure. The amplitude of scattering wave increases as the dissipation factor increases. Last but not least, the recursive method is efficient in calculating the scattering cross section and used to design a scattering-cancellation-type invisibility cloak.

References

[1] Pendry J B, Schurig D and Smith D R 2006 *Science* **312** 1780
[2] Cummer S A and Schurig D 2007 *New J. Phys.* **9** 45
[3] Cheng Y, Yang F, Xu J Y and Liu X J 2008 *Appl. Phys. Lett.* **92** 151913
[4] Cummer S A, Popa B I, Schurig D, Smith D R, Pendry J, Rahm M and Starr A 2008 *Phys. Rev. Lett.* **100** 024301
[5] Guild M D, Haberman M R and Alù A 2010 *J. Acoust. Soc. Am.* **128** 2374
[6] Zhang S, Xia C and Fang N 2011 *Phys. Rev. Lett.* **106** 024301
[7] Cai L, Wen J H, Yu D L, Lu Z M and Wen X S 2014 *Chin. Phys. Lett.* **31** 094303
[8] Gao D B and Zeng X W 2012 *Chin. Phys. Lett.* **29** 114302
[9] Ying C and Liu X J 2009 *Chin. Phys. Lett.* **26** 153
[10] Lai Y, Chen H, Zhang Z Q and Chan C 2009 *Phys. Rev. Lett.* **102** 093901
[11] Fang N, Xi D, Xu J, Ambati M, Srituravanich W, Sun C and Zhang X 2006 *Nat. Mater.* **5** 452
[12] Yang Z, Mei J, Yang M, Chan N H and Sheng P 2008 *Phys. Rev. Lett.* **101** 204301
[13] Fok L and Zhang X 2011 *Phys. Rev. B* **83** 214304
[14] Zhang Z, Li R Q, Liang B, Zou X Y and Cheng J C 2015 *Chin. Phys. B* **24** 024301
[15] Ke M Z, Qiu C Y, Peng S S and Liu Z Y 2012 *Physics* **41** 663 (in Chinese)
[16] Zhu X, Liang B, Kan W, Zou X and Cheng J 2011 *Phys. Rev. Lett.* **106** 014301
[17] Cai C, Zhu X F, Xu T, Zou X Y, Liang B and Cheng J C 2015 *Ann. Phys.* (New York) **358** 83
[18] Zhu X F, Zou X Y, Zhou X W, Liang B and Cheng J C 2012 *Chin. Phys. Lett.* **29** 014102
[19] Xu T, Zhu X F, Liang B, Li Y, Zou X Y and Cheng J C 2012 *Appl. Phys. Lett.* **101** 033509
[20] Cai L W and Sanchez-Dehesa J 2007 *New J. Phys.* **9** 450
[21] Cai L W and Sanchez-Dehesa J 2008 *J. Acoust. Soc. Am.* **124** 2715
[22] Yuan L Y, Xiang Y, Lu J and Jiang H H 2015 *Chin. Phys. B* **24** 124301
[23] Zhang S, Zhang Y and Gao X W 2014 *Chin. Phys. B* **23** 124301